

## Lagrangian avenues of transport in the Earth's mantle

Judit Schneider

*Alfred Wegener Institute for Polar and Marine Research, Columbusstrasse, 27568 Bremerhaven, Germany*

Joerg Schmalz

*Institute for Geophysics, Westfälische Wilhelms-Universität, D-48149 Münster, Germany*

Tamás Tél

*Institute for Theoretical Physics, Eötvös University, Pf. 32, H-1538 Budapest, Hungary*

(Received 22 May 2007; accepted 17 July 2007; published online 14 September 2007)

A method of visualizing and characterizing stirring structures of high Rayleigh number geophysical flows whose time dependence is strongly aperiodic is presented. To this end, the system is leaked by defining a smaller region of the flow, so that a particle is considered to be escaped if it enters this region. By means of an ensemble of nonescaped tracers, we are able to characterize stirring and transport processes by visualizing the converging and stretching filamentations (stable and unstable manifolds) in the flow. The method indicates that the present-day Earth's mantle is not well stirred because the time that has passed since the formation of the Earth has not been long enough for the flow of the mantle to generate efficient stirring, and observations reveal indeed the existence of reservoirs of different materials. © 2007 American Institute of Physics. [DOI: 10.1063/1.2771416]

Chaotic advection has widely been studied in recent years.<sup>1-5</sup> The basic dynamical mechanism responsible for advective chaos is the time dependence of spatially smooth velocity fields.<sup>6,7</sup> The resulting Lagrangian dynamics can be made visible by tracer particles, treated as pointlike particles.<sup>1</sup> To visualize these otherwise hidden advection patterns in closed flows, the method of leaking<sup>8-11</sup> has been applied to a variety of two- and three-dimensional time-periodic flows (and to a problem of celestial mechanics<sup>12,13</sup>). The method is based on the idea of considering a subregion of the flow and investigating how Lagrangian particle trajectories escape from or enter into it, to provide a kind of fingerprint of the original advection dynamics. Here we extend these studies to aperiodic, long-lasting (briefly chaotically time-dependent) flows in which no invariant sets exist in a strict sense. Analogs of them can, however, be defined based on the concept of random maps.<sup>14-16</sup> Two sets of filamentation are shown to be present, namely converging and stretching ones, which we shall call stable and unstable manifolds for simplicity. The question is, how can these manifolds be visualized by means of the leaking method in chaotically time-dependent closed flows, and how can they be used to characterize stirring properties in the system? We consider a flow of geophysical relevance: a two-dimensional Rayleigh-Bénard convection. For large Rayleigh number and infinite Prandtl number, this flow is a good model of the vigorously convecting Earth mantle.

### I. INTRODUCTION

Geochemical observations from oceanic island basalts (OIB's) and midocean ridge basalts (MORB's) reveal that the Earth's mantle is heterogeneous in composition on different length scales<sup>17,18</sup> and that these heterogeneities must have

existed for a long time. In contradiction to these findings are recent seismic measurements that show that convection and stirring takes place throughout the mantle. Also, quantitative stirring studies seem to indicate that the present-day Earth's mantle is convecting vigorously enough to erase initial heterogeneities well within the age of the Earth.<sup>19,20</sup> The major question that arises is how the existence of heterogeneities can be reconciled with findings of a vigorously convecting mantle. Models have been proposed by Becker,<sup>21</sup> who considers blobs of geochemically different material that are advected by the flow. Most models favor, however, some form of geochemical layering in the lower mantle.<sup>22</sup> The proposed scenarios are often accompanied by two-dimensional (2D) numerical simulations that start from a given set of initial conditions that the authors consider feasible for the Earth's mantle. A potential problem with the stirring models that try to explain the geochemical evolution is the arbitrary choice of the initial heterogeneity. Because the stirring properties of convective flow vary strongly in space, this can potentially result in misleading stirring rates. The method of leaking to characterize stirring by chaotic advection is beneficial since it can be used to visualize regions of poor stirring.

For time-periodic flows, there are Kolmogorov-Arnold-Moser islands within the flow, coexisting with strongly stirred regions. In the context of geophysics, such structures have been found by Perugini,<sup>3</sup> examining the state of frozen lava flows on small scales (meters). The origin of the badly stirred islands is either the presence of regions of quasiperiodic (nonchaotic) advection<sup>1</sup> or the finite lifetime of the flow (fluid motion stops after some time).<sup>23,24</sup> In a long-lasting flow whose time dependence itself is chaotic, such transport barriers cannot be present.<sup>25</sup> Then, all structures will be smeared out and disappear on sufficiently long scales. The advection dynamics is area- or volume-preserving and the asymptotic distribution of tracers in such systems is

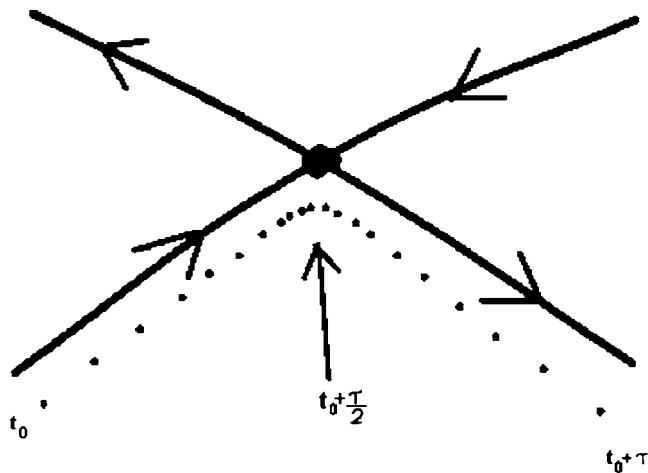


FIG. 1. Schematic illustration of the motion of a particle in a chaotic system consisting of hyperbolic fixed points with a stable and unstable manifold. For clarity, only a single hyperbolic point is indicated. A particle being close to the stable manifold at time  $t_0$  will be attracted by the hyperbolic fixed point along the stable manifold, being closest to the hyperbolic point at time  $t_0 + \tau/2$ . Then, it will be repelled from the hyperbolic fixed point along the unstable manifold ( $t_0 + \tau$ ).

uniform.<sup>6</sup> Stirring in this case is expected to be efficient. We will visualize dynamical stirring structures of the flow to show that, in spite of the chaotic time dependence of the flow, badly mixed regions do exist in which chemical heterogeneities could survive for a long time well within the Earth’s age.

The paper is organized as follows: In Sec. II, the method of leaking is reviewed. In Sec. III, we present the two-dimensional mantle convection model solved numerically and the results of our leaking analysis for visualizing the stirring properties. Section IV contains a discussion and our conclusions.

## II. THE LEAKING METHOD

The idea is to make Lagrangian structures visible, which have definite dynamical meanings: lines of intense stretching and lines of convergence. These lines are tangent to the eigenvectors corresponding to the positive and negative Lyapunov exponents of the tracer dynamics and provide the unstable and the stable foliation, respectively.<sup>26,27</sup> These lines are present in any flow generating chaotic advection, but in closed flows, i.e., flows in a fixed region from which no escape is possible, both types of them are fully space filling, and hence do not appear as clearly visible spatial structures.

To visualize the Lagrangian filamentation in closed flows, the leaking method considers a finite preselected region obtained by subtracting the leak from the full closed-flow region. The flow in this preselected region is consequently open. We specify trajectories out of an ensemble of tracers that do not leave this region within a time interval ( $t_0 < t < t_0 + \tau$ ), where  $t_0$  is an arbitrary initial moment and  $\tau$  is a time span definitely longer than the natural time scale of the flow.<sup>9</sup> The initial ( $t=t_0$ ) positions of these trajectories define the location of long lifetimes in the preselected region, and hence the stable manifold<sup>28</sup> (see the schematic Fig. 1).

The final ( $t=t_0 + \tau$ ) positions of the same trajectories fall on curves along which trajectories are about to escape the preselected region. They correspond to the unstable manifold. The midpoints ( $t=t_0 + \tau/2$ ) of the trajectories must be close to tracer positions that never escape the region<sup>28</sup> (both forward and backward in time). This set is called a chaotic saddle. It consists of an infinite number of hyperbolic points, each of them possessing a stable and an unstable manifold. The stable manifold (converging filament) is the set of initial points from which the given hyperbolic point can be reached. The unstable manifold (stretching filament) is the curve along which points from a close neighborhood of the hyperbolic points leave the point.

A good guess for an appropriate value of  $\tau$  is the average lifetime of chaos in the leaked flow. The particular value might also depend on the precise shape and location of the leak (for a discussion, see Schneider *et al.*<sup>8</sup>).

In strictly time-periodic flows, the chaotic saddle and its manifolds change within the period of the flow but are invariant on a stroboscopic picture taken with the period. In flows with nonperiodic (quasiperiodic or chaotic) time dependence and with smooth space dependence of the velocity field, recent theories<sup>14–16</sup> predict that the same objects remain well defined (although not invariant on any snapshot) and their fractal dimension is independent of the time ( $t_0$  and  $\tau$ ) of observation (provided the latter is sufficiently large).

In any case, the actual shape (and dimension) of these objects does depend on the choice of the preselected region (the choice of the leak), but any filament of them is an exact part of the original closed system’s filamentation. Thus, by selecting larger and larger regions (smaller and smaller leaks), a convergence toward the full filamentation can be seen. So, for any sufficiently large region, a faithful approximant of the closed system’s stretching and converging directions can be obtained. These filaments clearly define the stable and unstable directions around a given point of the leaked flow, but the same foliation characterizes the closed flow too, at the same point. On the other hand, with large leaks one gets insight into the local transport properties of the preselected region.

## III. MODEL AND RESULTS

Convection in a very viscous incompressible flow is defined by the conservation laws for mass, momentum, and energy,<sup>29,30</sup>

$$\nabla \underline{u} = 0, \quad \eta \nabla^2 \underline{u} + \rho \underline{g} = \nabla p, \quad \frac{\partial T}{\partial t} + \underline{u} \nabla T = \kappa \nabla^2 T.$$

Here  $\underline{u}$  is the velocity field, and  $\rho$ ,  $p$ , and  $T$  are the density, the pressure, and the temperature, respectively.  $\underline{g}$  denotes the acceleration due to gravity in the  $z$  direction, and  $\eta$  and  $\kappa$  stand for the dynamical viscosity and the thermal diffusivity, respectively. We assume an incompressible Boussinesq fluid with constant physical properties, except that density is linearly dependent on temperature,

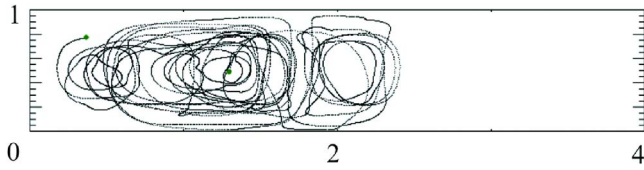


FIG. 2. Chaotic particle trajectory for a tracer started at  $x=1.3, y=0.5$  simulated over 20 overturns, about  $2 \times 10^{-2}$  dimensionless time units, at  $Ra = 10^7$ . There are two convection cells present in the flow whose precise shape is changing all the time. The particle shown leaves the left cell for shorter periods only.

$$\rho = \rho_0 [1 - \alpha(T - T_0)],$$

where  $\rho_0$  is the density at  $T=T_0=0$  and  $\alpha$  is the coefficient of thermal expansion. The equations are nondimensionalized by the depth scale  $d$ , the temperature scale  $\Delta T$ , and the time scale  $d^2/\kappa$ . The basic dimensionless number is then the Rayleigh number

$$Ra = \frac{\rho g \alpha \Delta T d^3}{\kappa \eta}$$

with  $\Delta T$  being the temperature difference between upper and lower surfaces. Internal heating is assumed to be negligible.

The thermal convection is studied in a two-dimensional rectangular domain with an aspect-ratio of 4. We use data characteristic of the Earth’s mantle: a Rayleigh number of  $Ra=10^7$  and an infinite Prandtl number ( $\nu/\kappa \rightarrow \infty$ ). Stress-free boundary conditions are applied. Therefore, on horizontal and vertical bounding surfaces, the normal component of velocity and the tangential components of traction are set to zero. The side walls are insulating and the top and bottom surfaces are set to the constant nondimensional temperatures 0 and 1, respectively.

In the numerical simulations, a primitive variable formulation was used. The method is closely related to the method described in Trompert and Hansen.<sup>31</sup> The code compares well with the benchmark results published in Blankenbach *et al.*<sup>32</sup> The resolution of the model consists of  $50 \times 254$  elements with grid refinements at the top and bottom boundaries in order to resolve the thin boundary layers.

Velocity components  $u$  and  $v$  are obtained on a regular mesh at discrete time levels  $t_i = i\Delta t, i=1, 2, \dots$  with a time step  $\Delta t = 2.1 \times 10^{-6}$ . The Lagrangian particle paths are calculated by post-processing the velocity data from the model to obtain particle locations from time level  $t_i$  to time level  $t_{i+1}$ , using the interpolated velocity fields  $u(x, y, t), v(x, y, t)$  at intermediate times  $t$ . The advection equations

$$\frac{dx}{dt} = u(x, y, t), \quad \frac{dy}{dt} = v(x, y, t)$$

were solved by means of a fourth-order Runge-Kutta method. The accuracy of calculated tracer paths is discussed by Schmalzl *et al.*<sup>33</sup> In time-dependent flows, the solution of these equations is typically chaotic. Figure 2 exhibits a typical particle trajectory. In the following droplet simulations, up to 300 000 particles will be used.

In *closed* chaotic flows, dye will be spread homogeneously over two-dimensional regions after some transient

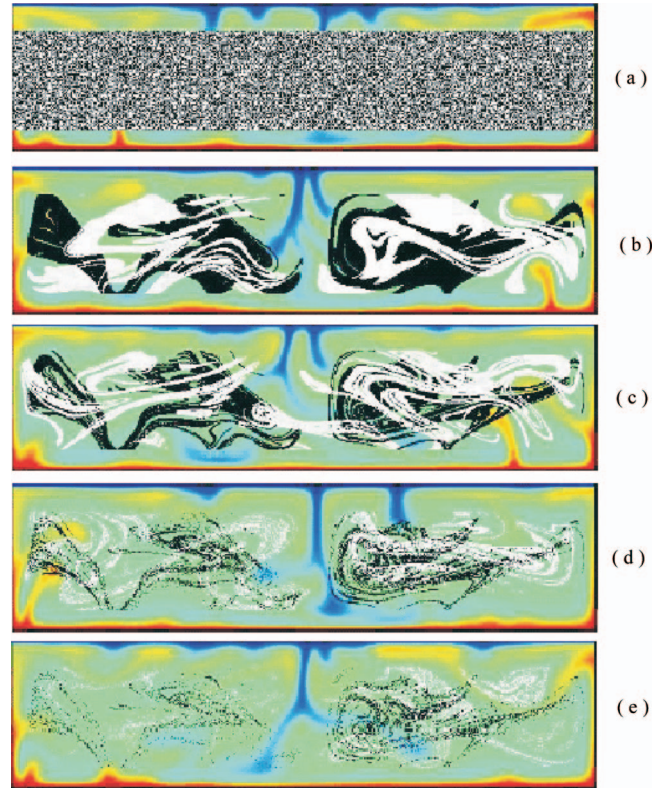


FIG. 3. (Color) Sequence of snapshots of the temporal evolution of passive particles in a domain with two convection cells. Panel (a) shows a preselected rectangle (dotted subregion) initially homogeneously filled with tracers. Subsequent panels depict the evolution of the tracers, showing the actual positions of the tracers in white, their initial positions in black. Panels (b)–(d) are taken at time instants after 2 (b), 6 (c), 14 (d), and 17 (e) average overturns of the cells. Color coding corresponds to rainbow-coloring from nondimensionalized temperatures of 0 at the top (dark blue), 0.5 (green), to 1 at the bottom (red) ( $Ra=10^7$ ).

time. Applying the method of leaking as described, we are able to visualize the dynamical structures of the system and to identify regions with low/high stirring rates. Therefore, a rectangular region is defined inside the flow in which idealized tracer particles are initially homogeneously distributed as shown in Fig. 3: particles that cross the borders of the rectangular region outward will be treated as escaped ones and are taken out of the system. In this way, the formerly closed system is opened up by leaking, and an escape of particles is possible.

Figure 3 shows a sequence of plots representing the set of initial (black) and final (white) positions of trajectories that did not leave the preselected region over time  $\tau$  for increasing values of the time span  $\tau$ . The flow is markedly aperiodic, which can clearly be seen in the temperature field, which is color-coded in the background of Fig. 3. The flow pattern is that of a two-cell problem since most of the time two convection cells exist, in which the location of the wall between the cells moves chaotically in time, generating cross-cell stirring.

White points, representing the actual position of the tracers at time  $\tau$ , accumulate along the main transport direction (unstable manifold). The longer the simulated time  $\tau$ , the more particles leave the rectangle, thus more and more “stripes” appear in the initially homogeneous (black) distri-

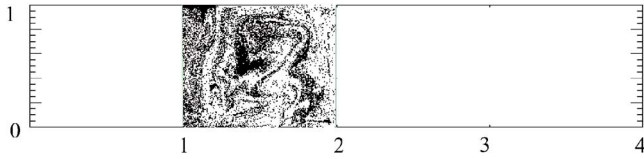


FIG. 4. Stirring of tracers out of a box, showing the initial positions of particles leaving the box toward the left (black) and toward the right (white) within ten overturns. The flow is the same as in Fig. 3, and the initial velocity field is that of Fig. 3(a).

bution. (The loss of structures over very long times is due to the finite number of particles used in the simulation.) The set of black points, representing the initial positions of the particles with the white end points, becomes more and more rarified and filamentary with increasing time. This evolution is similar to gradually removing the flesh from a backbone. The backbone, the asymptotic fractal shape, is the stable manifold of a never escaping set, the chaotic saddle, existing in the preselected rectangle.

Note, however, that the resulting distribution of tracer particles is not filamentary everywhere. There are some regions within the convection cells where tracers seem to accumulate. Especially in the right convection cell, there are some denser blobs (both in white and in black). Particles seem to be stirred faster in the left than in the right convection cell.

The region in between the convection cells and the regions around the side walls are regions of strong up- and down-welling, where the streamlines, which are similar to the temperature lines, are approximately vertical. In view of this, we can say that the Lagrangian patterns (the manifolds) have completely different structures from the Eulerian ones (the streamlines). In particular, the latter ones are not fractals. Nevertheless, there are some global relations between them. The stable manifold, for example, cannot penetrate the up- and down-welling regions [Figs. 3(b)–3(e)] since points initially situated there are quickly transported toward the horizontal walls (toward the leaks), and thus cannot remain in the preselected rectangle.

We can infer from the sequence of plots in Fig. 3 that stirring occurs mainly within each cell and cross-cell stirring is less dominant. In panel (c) we can see the less frequent situation where particles (white) are crossing the cells, corresponding to the results reported by Schmalzl.<sup>34</sup> It can also be seen in panel (c) that after six overturns, dense material blobs are still existing. The disappearance of these inhomogeneities takes around 17 overturns (e).

The stirring process of a smaller part of one convection cell with its surroundings is shown in Fig. 4. From the interwoven black and white structures, denoting the initial position of particles leaving the box to the left or to the right, respectively, it can clearly be seen that particles within that box become stirred vigorously. But note again that there exist some regions where the structures are more blob-like than filamentary.

Figure 5 helps to gain insight into the meaning of the (chaotically time-dependent) manifolds. Here again, a smaller preselected region, the starting box, is shown, but we

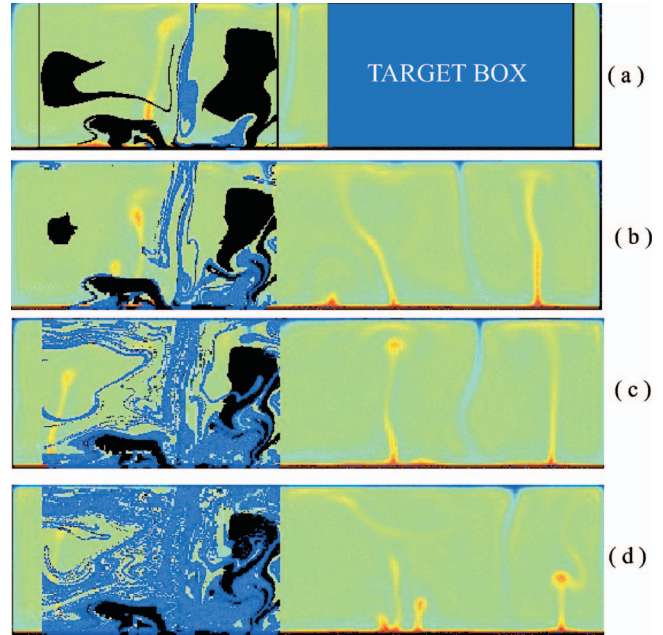


FIG. 5. (Color) Initial positions of particles in a box (left) that enter the right target box up to time  $\tau$  are shown in blue. Black points in the starting box denote locations wherefrom particles do not leave the starting box, i.e., they are badly stirred with their surroundings. In the subsequent panels, the time instants are approximately 16, 17, 18, and 20 large-scale convective overturns. Color coding is the same as in Fig. 3

have identified another box too (the target box), with the purpose of showing initial conditions of trajectories in the former box that enter the target box up to time  $\tau$  (these trajectories are then not followed any longer). The blue region, denoting the initial positions of particles that have reached the target box, increases as time goes on and comes close to the black filaments (denoting initial points wherefrom particles never leave the first box). The black filaments themselves become rarified with time, since the majority of the particles leave the starting box. After a very long time, the blue and black filamentary regions would become complementary sets of each other.

This numerical experiment can be seen as a simulation of the stirring of two spatially separated regions (starting and target region) with distinct material composition. It shows that two such reservoirs do mix (blue filaments), but there is the possibility that some material blobs remain over some time in their initial environment (black blobs). This indicates that particles *close* to the unstable manifold of the chaotic saddle existing within a box can quickly reach any other regions of the flow, whereas particles starting *on* the stable manifold stay in the preselected region in principle forever. Thus, nearby points can depart to large distances: a pair of points from which one is on the stable manifold and the other is somewhat off will deviate strongly. This all shows that stirring between the stable manifold (black) and its complement (blue) is strong.

The unstable manifold has the same property for the time-reversed particle motion. Thus, to a given point we can find another one so that they stay close to each other over their entire past only if the pair falls on the same filament of the unstable manifold. But a random choice of two nearby



FIG. 6. (Color) Color-coding of the residence time of particles of the box shown in Fig. 4. Depending on how long it takes for the particles to leave the box (how long it takes to mix with the surroundings), the initial positions are colored differently: black colors toward dark red denote initial positions wherefrom particles escape very rapidly; light red toward white mark initial positions where particles tend to stay a long time within the box. White colors denote places wherefrom particles do not leave the box during the simulation time (ten overturns).

points of the flow will provide us (with probability 1) with points whose past was drastically different.

Measuring the residence time, i.e., how long it takes for particles (initially homogeneously distributed in a chosen box) to leave the box, results in Fig. 6. Short residence times (black and dark red) stand for locations where particles escape rapidly out of the box. Positions with large residence times (light red and white) correspond to an approach toward one of the never-escaping orbits. Points with large residence times must therefore be close to the converging foliation, i.e., to the stable manifold. The average time  $\tau$  for a particle to leave the box, determined by the exponential decay of remaining particles  $N(t) = N(t_0)e^{-\gamma(t-t_0)}$ , follows from the escape rate  $\gamma = 810$  with  $\tau = 1/\gamma = 0,0012$ , corresponding to one or two overturns. In other words, a particle started in the region of Fig. 6 needs on average one or two overturns to get stirred with the box-surrounding material.

Note that light red and white spots in Fig. 6 mark regions wherefrom particles become stirred very slowly with their surroundings (here, particles starting from white places need more than ten overturns). Although particles are well stirred with their surroundings on average as shown, particles starting from these locations might survive for a longer (but limited) period as heterogeneous structures, like the ones found in field observations.<sup>3</sup>

In general, the stirring strength can be characterized by means of the fractal dimension of the stirring structures. Due to the topological invariance of the flow mentioned above, the fractal dimension  $D_0$  can be shown to remain unchanged.<sup>14–16</sup> The fact that the dimension of the once established pattern remains fixed is a crucial point for the ability of characterizing the strength of stirring processes: the

value of the fractal dimension is a measure of the stirring strength of the given preselected region.

By determining numerically the divergence rates of originally nearby particle pairs in the flow, we obtained an approximate value for the average Lyapunov exponent as  $\lambda = 1339$ , in dimensionless units. The approximate fractal dimension of the advection pattern of Fig. 6 follows from  $\gamma$  and  $\kappa$  via the Kantz-Grassberger relation<sup>35</sup> as  $D_0 \approx 2 - \gamma/\lambda = 1.4$ .

In general, in filamentary regions, stirring is stronger the smaller the deviation of the fractal dimension is from the full dimension of the system ( $D=2$ ), since strong stirring results from strong chaoticity (big Lyapunov exponents).

#### IV. CONCLUSION

In order to understand stirring properties in the Earth's mantle from a novel perspective, we applied the leaking method to visualize transport routes of the convection in a very viscous, temporally aperiodic flow. Using passive tracers, we identified basic local transport directions of the flow by showing the unstable manifolds. We confirm earlier observations<sup>34</sup> that stirring within convection cells operates on shorter time scales than stirring across convection cells.

Also, we characterized stirring of smaller regions with their surroundings with the help of the fractal dimension  $D_0$ . We found that the stirring strength is spatially inhomogeneous. In vigorously stirring (hyperbolic) flows, a fractal filamentation should be present everywhere. We found indications of this in Figs. 3–6. Within the well-stirred regions, however, some smaller domains exist that survive over a longer time span without being properly stirred with their surroundings. This could be seen in the figures, where some regions of a given color are more blob-like than filamentary. This result suggests that although we model the Earth's mantle as a vigorously convecting high Rayleigh number fluid, some heterogeneities may survive over a longer time period. In other words, heterogeneous regions do not necessarily have to have higher viscosities than the normal mantle<sup>36</sup> in order to survive until the present. Assuming an average overturn time between 400 and 500 million years, we showed that within the approximately ten overturns that have taken place until today, inhomogeneities were unable to mix intensively, and they are therefore still present in the Earth's mantle.

#### ACKNOWLEDGMENT

This research has been supported by the Hungarian Research Foundation (OTKA T047233 TS044839).

<sup>1</sup>J. M. Ottino, *The Kinematics of Mixing: Stretching, Chaos and Transport* (Cambridge University Press, Cambridge, UK, 1989).

<sup>2</sup>A. Huppert and L. Stone, *Am. Nat.* **152**, 447 (1998).

<sup>3</sup>D. Perugini, G. Poli, and G. D. Gatta, *Lithos* **65**, 313 (2002).

<sup>4</sup>D. Farmer, R. Pawlowicz, and R. Jiang, *Dyn. Atmos. Oceans* **36**, 43 (2002).

<sup>5</sup>T. Tél, A. de Moura, C. Grebogi, and G. Károlyi, *Phys. Rep.* **413**, 91 (2005).

<sup>6</sup>E. Ott, *Chaos in Dynamical Systems* (Cambridge University Press, Cambridge, UK, 1993).

<sup>7</sup>T. Tél and M. Gruiž, *Chaotic Dynamics* (Cambridge University Press, Cambridge, UK, 2006).

- <sup>8</sup>J. Schneider, T. Tél, and Z. Neufeld, *Phys. Rev. E* **66**, 066218 (2002).
- <sup>9</sup>J. Schneider and T. Tél, *Ocean Dyn.* **53**, 64 (2003).
- <sup>10</sup>J. Schneider, V. Fernández, and E. Hernández-García, *J. Mar. Syst.* **57**, 111 (2005).
- <sup>11</sup>I. Tuval, J. Schneider, O. Piro, and T. Tél, *Europhys. Lett.* **65**, 633 (2004).
- <sup>12</sup>J. Nagler, *Phys. Rev. E* **69**, 066218 (2004).
- <sup>13</sup>J. Nagler, *Phys. Rev. E* **71**, 026227 (2005).
- <sup>14</sup>J. Jacobs, E. Ott, T. Antonsen, and J. Yorke, *Physica D* **110**, 1 (1997).
- <sup>15</sup>Z. Neufeld and T. Tél, *Phys. Rev. E* **57**, 2832 (1998).
- <sup>16</sup>G. Károlyi, T. Tél, A. de Moura, and C. Grebogi, *Phys. Rev. Lett.* **92**, 174101 (2004).
- <sup>17</sup>S. R. Hart, *Nature (London)* **309**, 753 (1984).
- <sup>18</sup>A. W. Hofmann, *Nature (London)* **385**, 219 (1997).
- <sup>19</sup>U. Christensen, *Earth Planet. Sci. Lett.* **95**, 382 (1989).
- <sup>20</sup>N. R. A. Hoffman and D. P. McKenzie, *Geophys. J. R. Astron. Soc.* **82**, 163 (1985).
- <sup>21</sup>T. W. Becker, J. Kellogg, and R. J. O'Connell, *Earth Planet. Sci. Lett.* **171**, 351 (1999).
- <sup>22</sup>P. van Keken, C. Ballentine, and E. Hauri, "Geochemistry of the mantle and core," edited by R. Carlson, in *Treatise of Geochemistry* (Elsevier, Amsterdam, 2003), Vol. 2.
- <sup>23</sup>G. Haller and A. C. Poje, *Physica D* **119**, 352 (1998).
- <sup>24</sup>S. Wiggins, *Chaotic Transport in Dynamical Systems* (Springer, New York, 1992).
- <sup>25</sup>R. Pierrehumbert, *Chaos, Solitons Fractals* **4**, 1091 (1994).
- <sup>26</sup>M. M. Alvarez, F. J. Muzzio, S. Cerbelli, A. Adrover, and M. Giona, *Phys. Rev. Lett.* **81**, 3395 (1998).
- <sup>27</sup>M. Giona, A. Adrover, F. Muzzio, and S. Cerbelli, *Physica D* **132**, 298 (1999).
- <sup>28</sup>Y.-C. Lai, T. Tél, and C. Grebogi, *Phys. Rev. E* **48**, 709 (1993).
- <sup>29</sup>F. M. Richter, *J. Geophys. Res.* **78**, 8735 (1973).
- <sup>30</sup>D. P. McKenzie, J. M. Roberts, and N. O. Weiss, *J. Fluid Mech.* **62**, 465 (1974).
- <sup>31</sup>R. A. Trompert and U. Hansen, *Geophys. Astrophys. Fluid Dyn.* **83**, 261 (1996).
- <sup>32</sup>B. Blankenbach *et al.*, Convection Benchmark Working Group, *Geophys. J. Int.* **98**, 23 (1989).
- <sup>33</sup>J. Schmalzl, G. A. Houseman, and U. Hansen, *Phys. Fluids* **7**, 1027 (1995).
- <sup>34</sup>J. Schmalzl, *J. Geophys. Res.* **101**, 21847, DOI:10.1029/96JB01650 (1996).
- <sup>35</sup>H. Kantz and P. Grassberger, *Physica D* **17**, 75 (1985).
- <sup>36</sup>M. Manga, *Geophys. Res. Lett.* **23**, 403, DOI:10.1029/96GL00242 (1996).